RSC Advances

PAPER

View Article Online
View Journal | View Issue

Cite this: *RSC Adv.*, 2015, **5**, 50660

Towards mechanically robust cellulose fiber-reinforced polypropylene composites with strong interfacial interaction through dual modification†

Shuman Wang, Yifeng Lin, Xinxing Zhang* and Canhui Lu*

Received 29th January 2015
Accepted 1st June 2015

DOI: 10.1039/c5ra01792k

www.rsc.org/advances

Strong interfacial interaction between bamboo cellulose fiber (BCF) and a polymeric matrix is very important to improve the mechanical properties of cellulose fiber-reinforced polymeric composites. In this study, we developed an effective approach to enhance the interfacial adhesion through modifying both polypropylene (PP) and cellulose fiber. Maleic anhydride was mechanochemically grafted onto PP to achieve the interaction with the reactive hydroxyl groups on the surface of 2,2,6,6-tetramethylpiperidine-1-oxy radical (TEMPO)-oxidized bamboo cellulose fiber (TBCF). Fourier transform infrared spectra and X-ray diffraction analysis indicated the existence of strong interfacial interaction between TBCF and the modified PP matrix. It was further found by thermogravimetric analysis that about 5 wt% of PP formed a strong combining force with TBCF after melt compounding. The combination of mechanochemical modification of PP and TEMPO-mediated oxidation of BCF showed a synergistic effect on the tensile strength of the prepared composites. The tensile strength of modified PP/TBCF (50/50 wt%) composites prepared through dual modification was remarkably improved compared to those of neat PP/TBCF composites and modified PP/BCF composites, enhanced by about 112.4% and 53.8%, respectively.

1. Introduction

Cellulose is one of the most abundant, renewable and biodegradable natural polymers existing in wood, bamboo, cotton, hemp, straws, sugarcane bagasse and other plants.[1–3] Recently, the emphasis on sustainable and environmentally friendly materials has steered the trend of incorporating natural cellulose fiber into polymeric composites.[4–6] There are some problems faced by researchers in this field, most of them are related to the highly polar surface of cellulose, which causes its low interfacial compatibility with non-polar polymeric matrices and the ensuing fiber aggregation.[7] Numerous strategies have been developed to overcome these problems.[8] Typically, the use of coupling agents and the esterification of cellulose with fatty acids are two major approaches to improve interfacial interaction between cellulose and polymeric matrices.

In general, the Young's modulus of polymers can be increased by the reinforcement of cellulose, while the tensile strength does not improve or sometimes decreases due to the poor interfacial interaction even after modification.[9] For example, Qiu *et al.*[10] studied the effect of maleated polypropylene (MAPP) on the performance of polypropylene (PP)/cellulose composites. The addition of MAPP improved the interfacial adhesive between cellulose and PP matrix to some extent. But the tensile strength of the PP/cellulose (60/30 wt%) composites containing 10 wt% MAPP only slightly increased comparing with that of neat PP. Similarly, Mulinari *et al.*[11] reported that the incorporation of zirconium oxychloride-treated sugarcane bagasse cellulose had a negative effect on the tensile strength of high density polyethylene. This drawback was also proved by Fávaro *et al.*'s work.[12] The surface acetylation of rice husk fibers as a strategy produced polyethylene (PE)/rice husk composites with improved modulus, while the modified rice husk-filled composites showed lower tensile strength than that of neat PE.

To our best knowledge, modification of both cellulose and polymeric matrices has not been investigated in depth so far, as there are only limited reports about it. For example, Iwamoto *et al.*[13] realized homogeneous filler dispersion in the PP/cellulose composites with the combination of added MAPP and cellulose surface-coating, leading to higher Young's modulus and tensile strength than those of neat PP. However, harmful reagents (*e.g.* toluene) were repeatedly used in these pretreatments, which might hinder their large-scale applications.

In this work, we investigated that the synergistic effect of mechanochemical modification of PP and 2,2,6,6-tetramethylpiperidine-1-oxy radical (TEMPO)-mediated oxidation of cellulose

State Key Laboratory of Polymer Materials Engineering, Polymer Research Institute of Sichuan University, Chengdu 610065, China. E-mail: xxzwwh@126.com; canhuilu@scu.edu.cn; Fax: +86-28-85402465; Tel: +86-28-85460607

† Electronic supplementary information (ESI) available. See DOI: 10.1039/c5ra01792k

on the interfacial interaction and mechanical properties of PP/cellulose composites. Derived from the traditional Chinese stone-mill, the innovative pan-mill equipment is efficient in triggering mechanochemical reactions due to its three-dimensional scissor structure.[14–16] The self-designed pan-mill type mechanochemical reactor was employed to pulverize and modify the surface of PP powders simultaneously *via* mechanochemical reaction with maleic anhydride (MAH) in solid state. TEMPO-oxidization promoted cellulose fibrillation by selectively converting the surface hydroxyl moieties of cellulose into carboxylic groups and released reactive hydroxyl groups on the surface of cellulose, thereby enhancing the interfacial adhesion between cellulose and PP matrix. The synergistic effect of mechanochemically modified PP and TEMPO-oxidized bamboo cellulose fiber (TBCF) on the interfacial interaction between cellulose and PP matrix was examined. In contrast to the previous works[11,12,17] where cellulose rarely showed reinforcing effect on the tensile strength of polymeric composites, the prepared modified PP/TBCF composites with high filler loading (≥50 wt%) in this study showed a remarkably improved tensile strength comparing to that of neat PP due to the enhanced interfacial interaction. This new process is highly attractive and ready for large-scale applications.

2. Experimental

2.1 Materials

The raw material of bamboo cellulose fiber (BCF) with solid content of 28–32 wt% used in this study was supplied by Yongfeng Paper Co., China. PP homopolymer T30S was purchased from Lanzhou Petrochemical Industrial Company, China. It had a melting temperature of 165 °C and a melt flow index (MFI) of 3.2 g per 10 min (2.16 kg at 230 °C). The TEMPO, sodium bromide (NaBr), sodium hypochlorite (NaClO), MAH and dimethylbenzene were purchased from Chengdu Kelong Inc., China. All reagents were of analytical grade and distilled water was used for the preparation of all solutions.

2.2 Mechanochemical modification of PP *via* pan-milling

Mechanochemical modification of PP was performed using the pan-mill type mechanochemical reactor. The details of the pan-mill equipment and operation procedure were depicted in our previous publications.[18,19] Generally, a mixture of PP/MAH with weight ratio of 100/7.5 was fed into hopper set at the middle of the moving pan. Milled powder was discharged from the brim of the pans. The discharged powder was then collected for the next milling cycle. The whole milling process was conducted at a rotating speed of 60 rpm under ambient temperature. The obtained powder was Soxhlet extracted with water for 72 h to ensure thorough removal of residual MAH for subsequent analysis. Then, the modified PP powder product was dried in an electric oven at 60 °C. Neat PP pellets were milled at the same way as a comparison.

2.3 TEMPO-mediated oxidation of cellulose

BCF was pretreated by TEMPO-mediated oxidation method. NaBr (1 mmol per gram of cellulose) and TEMPO (0.1 mmol per gram of cellulose) were added to the suspension of bamboo pulp with the concentration of pulp in water was 2 wt%. Then NaClO (5 mmol per gram of cellulose) was added slowly to the suspension. The pH of the mixture was maintained to 10 at room temperature by adding 0.5 M sodium hydroxide (NaOH) and 0.5 M hydrochloric acid (HCl) while stirring the suspension. After all NaClO was consumed and pH kept still, the cellulose was washed thoroughly with deionized water until the filtrate solution was neutral. The products were filtered and dried at 60 °C in an electric oven to obtain the TBCF with about 30 wt% solid content.

The carboxylate content of the TBCF was determined by conductometric titration method.[20] The dry sample (1 g) was soaked in 100 mL 0.001 M sodium chloride solution in the presence of magnetic stirring, then added with 0.1 M HCl to set the pH value in the range of 2.5–3.0. A 0.1 M NaOH solution was added at the rate of 0.1 mL min^{-1} up to pH 11 by pH meter. The total content of the TBCF was calculated from:

$$\text{The carboxylate content (mmol g}^{-1}) = [(V_1 - V_0) \times C_{NaOH} \times 1000]/m_0$$

where V_1 and V_0 are the consumed volume of NaOH solution at the equivalent point, respectively, and m_0 is the weight of dried product.

2.4 Preparation of PP/cellulose composites

In order to investigate the interfacial interaction between cellulose and polymeric matrix, modified PP/TBCF (10–60 wt% related to total weight) composites were prepared. Meanwhile, neat PP/TBCF composites and modified PP/BCF composites were obtained as comparison. The cellulose fiber with about 30 wt% solid content and PP were premixed with a high speed agitator for uniform dispersion. The mixture was then kneaded by a twin-roller mixer Brabender Plasticorder (PLE-330, Brabender Co., Germany). Compounding was carried out for 20 min at a roller speed of 50 rpm at 180 °C, and water was removed at this stage. The melt compounded products were crushed into small pieces, then compressed at 180 °C and 10 MPa pressure for 8 min. A schematic illustration of the composite preparation method is shown in Fig. 1.

2.5 Characterization

2.5.1 Optical microscopy. The morphologies of the modified PP powders and the TBCF were observed using an optical microscope (Leica DMLM) and captured by a digital imaging system. The PP powders and TBCF were suspended in ethanol and water, respectively, both with a concentration of 0.5 wt%. One drop of the diluted sample was dropped on a glass slide and stamped with a coverslip for the observation.

2.5.2 X-ray photoelectron spectroscopy (XPS) analysis. To investigate the structure changes of PP during mechanochemically milling with MAH, the pan-milled PP powder was Soxhlet extracted with water for 72 h and then dried at 80 °C. The neat PP and modified PP powders were characterized by

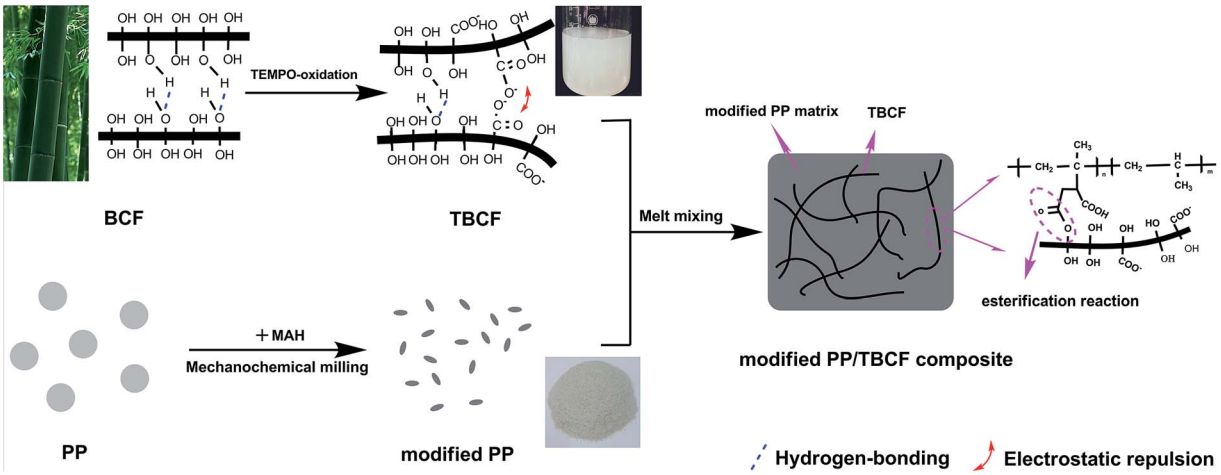

Fig. 1 Schematic illustration for the preparation of modified PP/TBCF composite through dual modification.

XPS (ESCALab220I-XL electron spectrometer from VG Scientific using 300 W AlKα radiation) for element and chemical analysis.

2.5.3 Measurement of grafting degree of the modified PP. The neat PP and modified PP powders were purified using a precipitation method. About 3 g of powders were dissolved into 100 mL of refluxing xylene and precipitated into 500 mL of acetone. Then filtered, washed by acetone for three times and dried at 80 °C for 12 h in an electric oven. The grafting degree of the purified product was determined by chemical titration.[21] The average data were obtained from three replicates.

2.5.4 Water-contact angle measurement. The hydrophilicities of the neat PP and modified PP membrane surface were characterized by water-contact angle measurement. A contact angle goniometer (OCA20, Dataphysics, Germany) equipped with a single-LED light source was used for imaging the liquid drop auto-dispersed on the sample surface. The drop image is then grabbed per 10 s to obtain dynamic contact angle data.

2.5.5 Fourier transform infrared spectroscopy (FTIR) analysis. PP/cellulose composites were extracted with boiling dimethylbenzene for 120 h to remove the matrix resin. The obtained cellulose powder samples were analyzed by FTIR (Nicolet 560 spectrometer, USA). The spectra were recorded from 4000 to 400 cm^{-1} at a resolution of 2 cm^{-1} over 20 scans. The samples were completely dried in an oven before tested.

2.5.6 Scanning electron microscopy (SEM) analysis. SEM (JSM-5900LV, JEOL) was employed to observe the morphology of cellulose in the composites. Standard specimens were cryogenically fractured in liquid nitrogen. Before observing, the fracture surface was sputter-coated with gold.

2.5.7 X-ray diffraction (XRD) analysis. XRD patterns were collected on a Philips Analytical X'Pert X-diffractometer (Philips Co., Netherlands), using Cu-Kα radiation ($k = 0.1540$ nm) at an accelerating voltage of 40 kV and the current of 40 mA. The data were collected from 2 = 5–60 with a step interval of 0.03°. The degree of crystallinity can be relatively expressed by the percentage crystallinity index (CrI). The equation used to calculate the CrI[22] was in the following form:

$$\mathrm{CrI} = [(I_{002} - I_{\mathrm{am}})/I_{002}] \times 100$$

I_{002} and I_{am} are the count reading at peak intensity at 2 close to 22° and 18°, representing crystalline part and amorphous part in cellulose, respectively.

2.5.8 Thermal analysis. Thermogravimetric analysis (TG) and derivative thermogravimetric analysis (DTG) were carried out with a TA-2000 analyzer (TA Instrument, USA) under nitrogen purge (flow rate about 100 mL min^{-1}). The scanning rate of 10 °C min^{-1} and temperature range of 30–600 °C was used. About 5 mg of samples were placed in an open alumina crucible for characterization. All the samples were oven dried at 60 °C for 24 h before testing.

2.5.9 Tensile tests. The stress–strain properties were measured according to the ASTM D 412-80 specification using dumb-bell test pieces on an Instron 5567 universal testing machine (Instron Co., Canton, USA) at a crosshead speed of 50 mm min^{-1}. At least five measurements for each sample were made in order to eliminate experimental error.

3. Results and discussion

3.1 Mechanochemical modification of PP

Surface-modified PP powders were prepared through solid-state pan-milling PP pellets with MAH under ambient temperature. Optical micrograph (Fig. 2a) reveals that the PP pellets are effectively pulverized into small particles with a particle size of 10 μm or less after 10 cycles of pan-milling. Furthermore, it acquired a rougher surface and a larger specific area after mechanochemical treatment, which would benefit its interfacial adhesion with fibers.[23]

The structure changes of PP before and after mechanochemical modification were characterized by XPS (as shown in Fig. 3). It can be seen that the oxygen content of modified PP surface is three times more than that of neat PP. The main peak appears at the binding energy of C 1s in $-CH_2-$ is about 284.9 eV. In Fig. 3d, a weak peak can be observed at the binding energy of 288.4 eV, which is ascribed to the –C=O bond.[24]

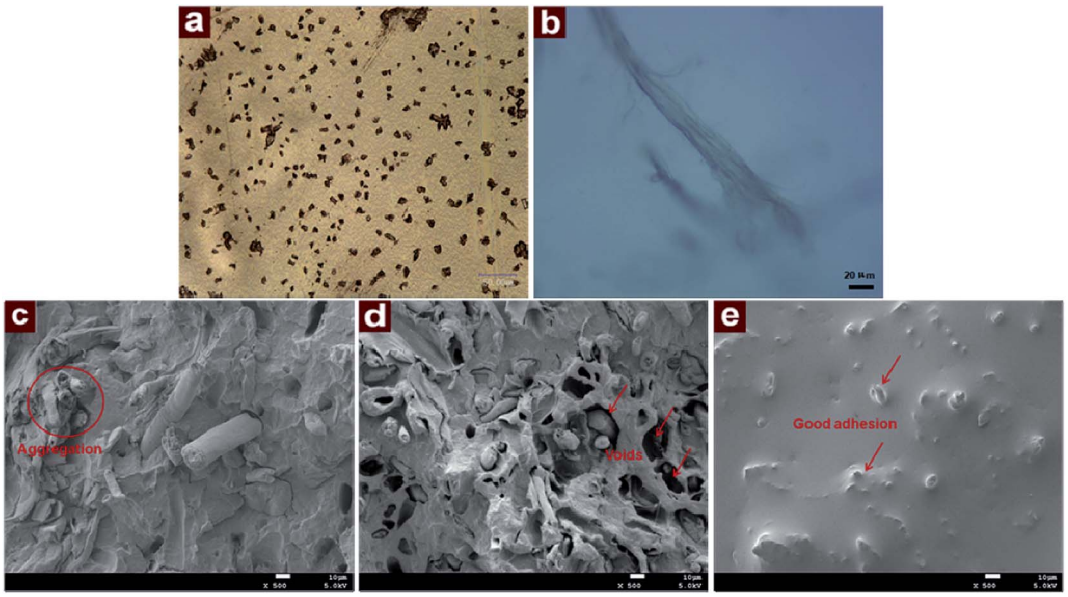

Fig. 2 Optical micrographs of modified PP powder (a), TBCF (b) and SEM images of neat PP/TBCF composite (c), modified PP/BCF composite (d) and modified PP/TBCF composite (e) with 30 wt% cellulose.

Meanwhile, the grafting degree of the mechanochemically modified PP was measured by chemical titration method. The experiments were performed in triplicate and the average value was measured to be 1.4%, indicating the high efficiency of mechanochemical modification. These results indicate that the macromolecular radicals of PP initiated graft polymerization reaction with low molecular MAH monomers due to the strong squeezing force in both radial and tangential directions exerted by the pan-mill equipment.[25,26]

The mechanochemical grafting of MAH onto PP may affect its polarity and hydrophilicity. Therefore, temperature-dependent contact angle measurements were carried out to investigate the variation of the surface hydrophilicity of PP. Fig. 4 shows the corresponding traces obtained for the dynamic contact angle measurements carried out with water placed on the surface of both samples. As expected, water wettability of PP increased after mechanochemical grafting of MAH due to the introduction of polar oxygen-contained groups. The mechanochemically modified PP presented a significantly higher level of water affinity than that of the neat PP. The average water contact angle at equilibrium of PP decreased from its original 113° to 90° after mechanochemical modification, indicating that the stress-induced mechanochemical modification of PP resulted in a more hydrophilic surface and hence improved its compatibilization with the polar cellulose.

3.2 Morphological development of PP/cellulose composites

In order to promote the interfacial interaction between cellulose and PP matrix, the BCF was pretreated with a TEMPO-mediated oxidation process. This process converted hydroxyl groups into carboxylic groups, generating electrostatic repulsion that favor the breakdown of the cohesion among the nanofibrils held by hydrogen bonding and released more reactive hydroxyl groups throughout the surface of cellulose.[27,28] The optical microphotograph of the TBCF is shown in Fig. 2b. The TBCF is swollen in water and some individual nanofibrils appear on the surface of fiber, indicating nanofibrils and aggregates were gradually loosened from the fiber surface after TEMPO-oxidation pretreatment. Similar results were reported by Saito *et al.*[29] and Chen *et al.*[30]

After TEMPO-oxidation pretreatment, the TBCF were melt-compounded with PP matrix in a melt mixer at 180 °C. The SEM images of the fractured surfaces of the composites with 30 wt% cellulose are shown in Fig. 2c–e, respectively. It can be seen from Fig. 2c that there are many pulled-out fibers in the fractured surface of neat PP/TBCF composites. Furthermore, the dispersion of TBCF are not uniform and aggregates of fibers can be found obviously in the neat PP matrix, indicating the poor interfacial compatibility of TBCF and neat PP matrix. In Fig. 2d, the interfacial boundary and the voids left on the fracture surface of modified PP/BCF composites are distinct. The large voids around the fibers demonstrate the weak adhesion at modified PP and BCF interfaces. It is apparent that the synergistic effect of the mechanochemically modified PP and TBCF improved the interfacial adhesion as the TBCF are almost completely embedded within the matrix (as shown in Fig. 2e). In addition, the TBCF are rather well distributed in the modified PP matrix. The same types of fracture surfaces were seen in the plasticized xylan/nanofibrillated cellulose composites, in which no nanofibrils were pulled out from the matrix during fraction due to the strong interfacial interaction between cellulose and matrix.[31]

3.3 Structure changes of cellulose before and after melt compounding

One of the primary purposes of this study is to evaluate the effect of mechanochemical modification on the interfacial

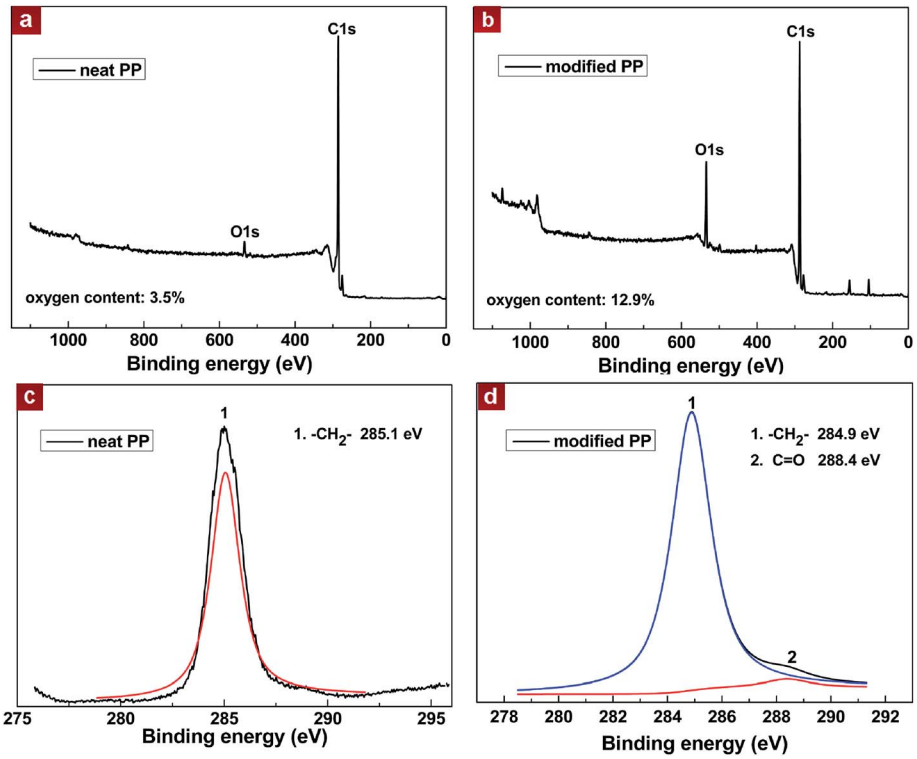

Fig. 3 XPS wide-scan and C 1s spectra of neat PP and modified PP.

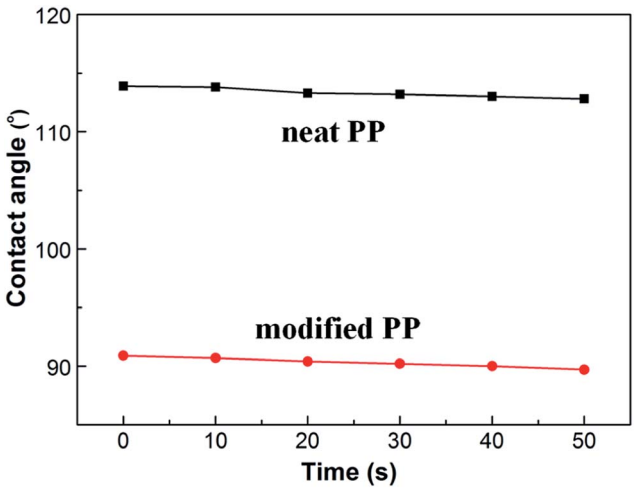

Fig. 4 Dynamic water contact angles of neat PP and modified PP.

interaction between PP and cellulose. In order to verify their strong interfacial adhesion, the structure changes of cellulose before and after melt compounding with PP were investigated in detail. The PP/cellulose composites were Soxhlet extracted for 120 h using dimethylbenzene as a solvent to ensure thorough removal of the PP resins in composites and then the obtained residue was collected for characterization.

Fig. 5 shows the FTIR spectra of TBCF (a), TBCF extracted from neat PP/TBCF composites (b) and modified PP/TBCF composites (c). All spectra are normalized to the reference peak at 1033 cm^{-1} which is assigned to C–O stretching vibration of the cellulose backbone.[32] The FTIR spectrum of TBCF extracted from neat PP/TBCF composites is almost the same as that of the original TBCF. However, it is very interesting to note that although the mechanochemically modified PP was removed in the same way as the neat PP, the FTIR spectrum of the TBCF extracted from modified PP/TBCF composites presents as a superposition of the FTIR curves of cellulose and PP. The strong and sharp adsorption peaks at 2917 and 1384 cm^{-1} are attributed to the CH_2 stretching vibration and methyl symmetric bending vibration of PP, respectively.[33] The results indicate that there are strong interfacial interactions between mechanochemically modified PP and TBCF after melt compounding.

The enhanced interfacial adhesion may be a result of the esterification reaction between MA moieties and hydroxyl groups on the surface of cellulose.[34–36] The TEMPO-mediated oxidation process contributed to the breakdown of intra- and intermolecular hydrogen bonds, releasing reactive hydroxyl groups on the surface of cellulose. Conductometric titration measurement indicates that the carboxylate content of TBCF is within the range of 0.8–1.0 mmol g^{-1}, confirming the generation of reactive hydroxyl groups. MA moieties of modified PP create chemical bonds with the exposed reactive hydroxyl groups on the surface of cellulose and establish strong interfacial interaction.

Fig. 6 presents the XRD patterns of TBCF (a), TBCF extracted from neat PP/TBCF composites (b), TBCF extracted from modified PP/TBCF composites (c) and BCF extracted from

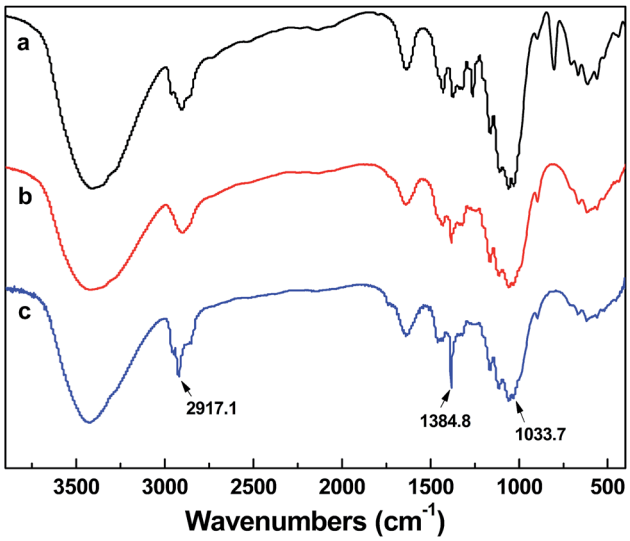

Fig. 5 FTIR spectra of TBCF (a), cellulose extracted from neat PP/TBCF composites (b) and modified PP/TBCF composites (c).

modified PP/BCF composites (d). All of the products maintained the original cellulose I crystal structure.[37] The crystallinity index of four kinds of cellulose is measured to be 79% (sample a), 80% (sample b), 77% (sample c) and 73% (sample d), respectively, using Segal's empirical method. The results indicate that the mechanical treatment caused little damage to the crystalline character of the cellulose during melt compounding. In addition, a new weak peak at $2\theta = 18.8°$ ascribing to the 130 plane of residual PP is observed in the spectrum of sample c.[38] This result further confirmed the strong interfacial interactions between the modified PP and TBCF.

The thermal properties of cellulose fibers is important to their applications in polymer composites, wherein the processing temperature for thermoplastic polymers is usually above 200 °C.[39] The melt compounded composites were etched by the Soxhlet extraction method using dimethylbenzene as solvent for 5 days to remove the PP matrix. The TG and DTG curves of TBCF (a), TBCF extracted from neat PP/TBCF composites (b), TBCF extracted from modified PP/TBCF composites (c), BCF extracted from modified PP/BCF composites (d) and neat PP (e) are shown in Fig. 7. As can be seen, the onset decomposition temperature of five samples is 287.4, 284.7, 284.9, 265.4 and 407.3 °C, respectively. The result indicates that the bamboo fiber used in this study has excellent thermal stability and its structure was not destroyed by the mechanical shearing during melt compounding, implying that the cellulose derived from this quickly grown plants is a promising inexpensive reinforcement for polymer composites. In comparison with sample b and d, the thermal degradation peak of residual PP at 400–480 °C can be clearly observed in the DTG curve of sample c, which is consistent with the thermal degradation temperature of neat PP (sample e). The amount of modified PP which has strong interactions with TBCF can be calculated from the TGA results. Cellulose was almost completely decomposed below 400 °C as shown in the TGA curves (sample a). Therefore, the approximately 5 wt% weight loss above 400 °C of the modified PP/TBCF composites (sample c) is attributed to the strongly combined PP onto TBCF after melt compounding, suggesting an enhanced interfacial adhesion between TBCF and modified PP matrix.

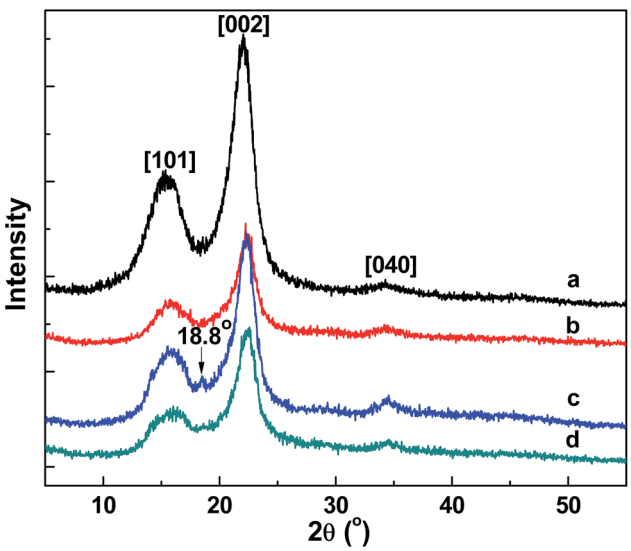

Fig. 6 XRD patterns of TBCF (a), TBCF extracted from neat PP/TBCF composites (b), TBCF extracted from modified PP/TBCF composites (c) and BCF extracted from modified PP/BCF composites (d).

In order to intuitively explain the aforementioned results, the SEM images of neat BCF, BCF extracted from modified PP/BCF composites and TBCF extracted from modified PP/TBCF composites are shown in Fig. 8. It is observed that the morphology of BCF extracted from modified PP/BCF composites is very similar to that of neat BCF (as shown in Fig. 8a). There is no residual PP on the surface of BCF which indicated the weak interfacial adhesion. However, Fig. 8c shows that a number of residual PP is adhered firmly on the surface of TBCF extracted from modified PP/TBCF composites, attributing to the strong interfacial interaction between modified PP and TBCF.

3.4 Mechanical properties of PP/cellulose composites

Typically, the enhanced interfacial interaction has a positive impact on the mechanical properties of PP/cellulose composites.[40] Since tensile strength is more dependent upon the polymer/cellulose interfacial interaction than tensile modulus,[41] the effect of mechanochemical modification and TEMPO-mediated oxidation on the tensile strength of PP/cellulose composites is shown in Fig. 9 and discussed in detail. The tensile strength of neat PP/TBCF composites dropped sharply with the increase of fiber loading due to the weak interfacial interaction between fiber and matrix.[42,43] In contrast, the tensile strength of modified PP/BCF composites improved obviously with the same fiber content. When the fiber content was increased, BCF was directly contact with one another and aggregated in the polymer matrix becoming fracture origins during mechanical testing. Islam *et al.*[44] reported that the tensile strength of the composites prepared from chemically

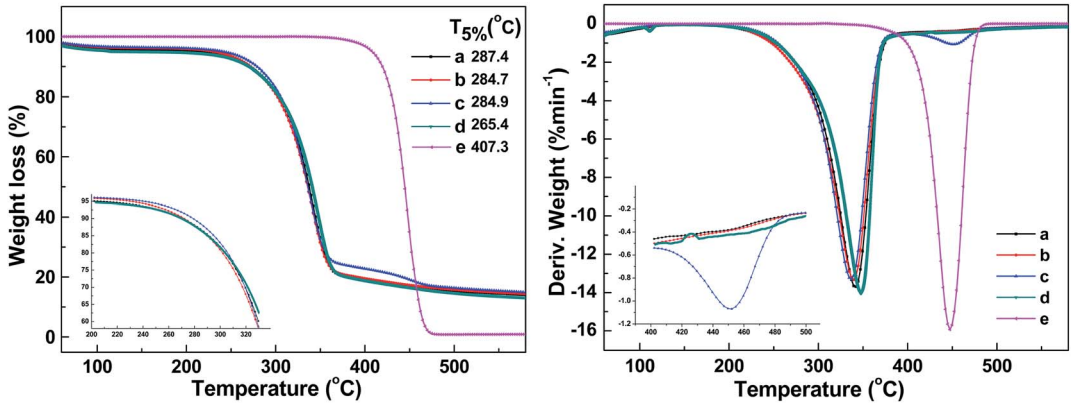

Fig. 7 TG and DTG curves of TBCF (a), TBCF extracted from neat PP/TBCF composites (b), TBCF extracted from modified PP/TBCF composites (c), BCF extracted from modified PP/BCF composites (d) and neat PP (e).

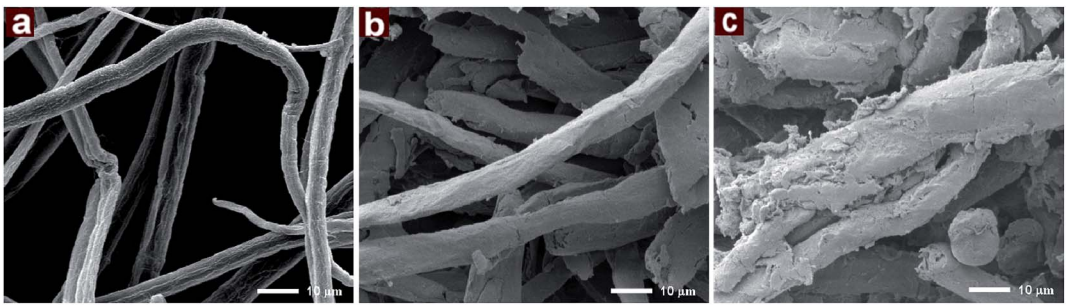

Fig. 8 The SEM images of neat BCF (a), BCF extracted from modified PP/BCF composites (b) and TBCF extracted from modified PP/TBCF composites (c).

treated coir decreased beyond 10 wt% fiber content. However, in our work, the tensile strength of modified PP/TBCF composites increased greatly and this effect is more evident at higher fiber content. The tensile strength of neat PP/TBCF and modified PP/BCF composites with 50 wt% cellulose is 21.8 and 30.1 MPa, while that of the modified PP/TBCF composite with 50 wt% cellulose is significantly increased to 46.3 MPa. The remarkable increase of tensile strength can be ascribed to the synergistic effect of the combination of mechanochemical modification of PP and TEMPO-mediated oxidation of cellulose. The MA moieties effectively bonded with the reactive hydroxyl groups on the cellulose surface, ensuring more efficient load transfer, thereby prevented crack growth and enhanced the mechanical properties.[45]

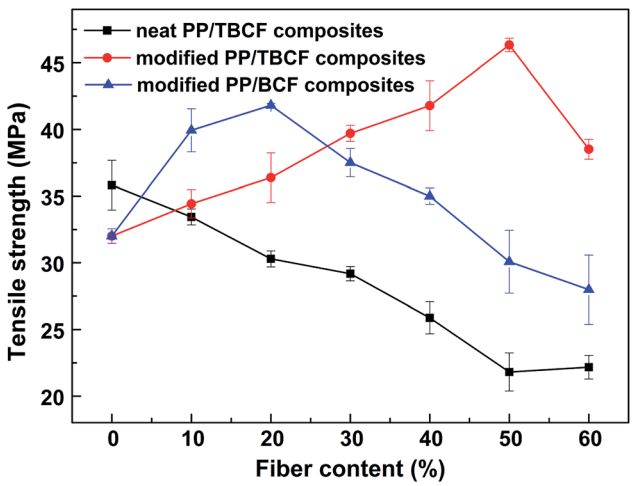

Fig. 9 Tensile strength of neat PP/TBCF, modified PP/TBCF and modified PP/BCF composites.

4. Conclusion

In this study, we demonstrated that the combination of the mechanochemical modification and TEMPO-mediated oxidation can be used as an effective approach to establish strong interfacial interaction between cellulose and PP matrix. The released reactive hydroxyl groups on the fiber surface generated by TEMPO-mediated oxidation processing effectively bonded with MAH-modified PP and thus created a strong interfacial adhesion. FTIR, XRD and TGA analysis indicated that approximately 5 wt% modified PP was tightly attached to TBCF and could not be removed even after 120 h of Soxhlet extraction by dimethylbenzene. The present investigation showed the feasibility of producing high performance cellulose fiber-reinforced polymer composites with remarkably

improved mechanical properties, which can have potential applications in the near future.

Acknowledgements

The authors would like to thank the National Science Foundation of China (51473100 and 51203105) and State Key Laboratory of Polymer Materials Engineering (Grant no. sklpme2015-3-04) for financial support.

References

1 P. R. Charani, M. Dehghani-Firouzabadi, E. Afra, A. Blademo, A. Naderi and T. Lindström, *Cellulose*, 2013, **20**, 2559–2567.
2 J. Li, X. Wei, Q. Wang, J. Chen, G. Chang, L. Kong, J. Su and Y. Liu, *Carbohydr. Polym.*, 2012, **90**, 1609–1613.
3 U. Ratanakamnuan, D. Atong and D. Aht-Ong, *Carbohydr. Polym.*, 2012, **87**, 84–94.
4 I. F. Pinheiro, A. R. Morales and L. H. Mei, *Cellulose*, 2014, **21**, 4381–4391.
5 X. Xiao, S. Lu, B. Qi, C. Zeng, Z. Yuan and J. Yu, *RSC Adv.*, 2014, **4**, 14928–14935.
6 M. Zhou, J. Yan, Y. Li, C. Geng, C. He, K. Wang and Q. Fu, *RSC Adv.*, 2013, **3**, 26418–26426.
7 S. Y. Lee, S. J. Chun, G. H. Doh, I. A. Kang, S. Lee and K. H. Paik, *J. Compos. Mater.*, 2009, **43**, 1639–1657.
8 S. Virtanen, J. Vartianen, H. Setälä, T. Tammelin and S. Vuoti, *RSC Adv.*, 2014, **4**, 11343–11350.
9 M. M. Ibrahim, W. K. El-Zawawy and M. A. Nassar, *Carbohydr. Polym.*, 2010, **79**, 694–699.
10 W. Qiu, F. Zhang, T. Endo and T. Hirotsu, *Polym. Compos.*, 2005, **26**, 448–453.
11 D. R. Mulinari, H. J. C. Voorwald, M. O. H. Cioffi, M. L. C. da Silva, T. G. da Cruz and C. Saron, *Compos. Sci. Technol.*, 2009, **69**, 214–219.
12 S. L. Fávaro, M. S. Lopes, A. G. Vieira de Carvalho Neto, R. Rogério de Santana and E. Radovanovic, *Composites, Part A*, 2010, **41**, 154–160.
13 S. Iwamoto, S. Yamamoto, S. H. Lee and T. Endo, *Composites, Part A*, 2014, **59**, 26–29.
14 D. Tian, X. Zhang, C. Lu, G. Yuan, W. Zhang and Z. Zhou, *Cellulose*, 2014, **21**, 473–484.
15 X. Zhang, Z. Lu, D. Tian, H. Li and C. Lu, *J. Appl. Polym. Sci.*, 2013, **127**, 4006–4014.
16 Z. Zhou, X. Zhang, D. Tian, R. Xiong and C. Lu, *Mater. Res. Innovations*, 2013, **17**, 84–91.
17 A. K. Bledzki, A. A. Mamun, M. Lucka-Gabor and V. S. Gutowski, *eXPRESS Polym. Lett.*, 2008, **2**, 413–422.
18 X. Zhang, C. Lu and M. Liang, *J. Appl. Polym. Sci.*, 2007, **103**, 4087–4094.
19 X. Zhang, C. Chen and C. Li, *Prog. Rubber, Plast. Recycl. Technol.*, 2012, **28**, 81–93.
20 T. Saito and A. Isogai, *Biomacromolecules*, 2004, **5**, 1983–1989.
21 C. Li, Y. Zhang and Y. Zhang, *Polym. Test.*, 2003, **22**, 191–195.
22 L. G. J. M. A. Segal, J. J. Creely, A. E. Martin and C. M. Conrad, *Text. Res. J.*, 1959, **29**, 786–794.
23 X. He, X. Zhang, W. Zhang, D. Tian and C. Lu, *J. Vinyl Addit. Technol.*, 2014, **20**, 177–184.
24 M. A. Chen, H. Z. Li and X. H. Zhang, *Int. J. Adhes. Adhes.*, 2007, **27**, 175–187.
25 X. Zhang, C. Lu and M. Liang, *J. Polym. Res.*, 2009, **16**, 411–419.
26 X. Zhang, C. Lu, Q. Zheng and M. Liang, *Polym. Adv. Technol.*, 2011, **22**, 2104–2109.
27 T. Saito, M. Hirota, N. Tamura, S. Kimura, H. Fukuzumi, L. Heux and A. Isogai, *Biomacromolecules*, 2009, **10**, 1992–1996.
28 A. Isogai, T. Saito and H. Fukuzumi, *Nanoscale*, 2011, **3**, 71–85.
29 T. Saito, S. Kimura, Y. Nishiyama and A. Isogai, *Biomacromolecules*, 2007, **8**, 2485–2491.
30 W. Chen, K. Abe, K. Uetani, H. Yu, Y. Liu and H. Yano, *Cellulose*, 2014, **21**, 1517–1528.
31 N. M. L. Hansen, T. O. J. Blomfeldt, M. S. Hedenqvist and D. V. Plackett, *Cellulose*, 2012, **19**, 2015–2031.
32 M. O. Adebajo and R. L. Frost, *Spectrochim. Acta, Part A*, 2004, **60**, 2315–2321.
33 H. Xia, Q. Wang, K. Li and G. Hu, *J. Appl. Polym. Sci.*, 2004, **93**, 378–386.
34 H. S. Yang, H. J. Kim, H. J. Park, B. J. Lee and T. S. Hwang, *Compos. Struct.*, 2007, **77**, 45–55.
35 L. M. Matuana, J. J. Balatinecz, R. N. S. Sodhi and C. B. Park, *Wood Sci. Technol.*, 2001, **35**, 191–201.
36 M. Kazayawoko, J. J. Balatinecz and R. T. Woodhams, *J. Appl. Polym. Sci.*, 1997, **66**, 1163–1173.
37 S. Alila, I. Besbes, M. R. Vilar, P. Mutjé and S. Boufi, *Ind. Crops Prod.*, 2013, **41**, 250–259.
38 M. R. Meng and Q. Dou, *Mater. Sci. Eng., A*, 2008, **492**, 177–184.
39 J. Wang, Q. Cheng, L. Lin and L. Jiang, *ACS Nano*, 2014, **8**, 2739–2745.
40 N. Lin, S. Wei, T. Xia, F. Hu, J. Huang and A. Dufresne, *RSC Adv.*, 2014, **4**, 49098–49107.
41 L. Zhong, S. Fu, X. Zhou and H. Zhan, *Composites, Part A*, 2011, **42**, 244–252.
42 M. M. Haque, M. Hasan, M. S. Islam and M. E. Ali, *Bioresour. Technol.*, 2009, **100**, 4903–4906.
43 X. Colom, F. Carrasco, P. Pages and J. Canavate, *Compos. Sci. Technol.*, 2003, **63**, 161–169.
44 M. N. Islam, M. R. Rahman, M. M. Haque and M. M. Huque, *Composites, Part A*, 2010, **41**, 192–198.
45 K. B. Adhikary, S. Pang and M. P. Staiger, *Composites, Part B*, 2008, **39**, 807–815.